Deuterium retention and ammonia production from D-implanted 316 L stainless steel: insights for future fusion reactors

T Aissou, F Ghiorghiu, Marco Minissale, T Angot, Gregory de Temmerman, Régis Bisson

PAPER • OPEN ACCESS

Deuterium retention and ammonia production from D-implanted 316 L stainless steel: insights for future fusion reactors

To cite this article: T Aissou *et al* 2024 *Mater. Res. Express* **11** 026510

Materials Research Express

PAPER

Deuterium retention and ammonia production from D-implanted 316 L stainless steel: insights for future fusion reactors

T Aissou[1], F Ghiorghiu[1], M Minissale[1], T Angot[1], G De Temmerman[2,3,4] and R Bisson[1]

[1] Aix-Marseille Univ, CNRS, PIIM, UMR 7345, Marseille, France
[2] ITER Organization, St. Paul Lez Durance Cedex, France
[3] Quadrature Climate Foundation, London, United Kingdom
[4] MINES ParisTech, University PSL, Institute of Higher Studies for Innovation and Entrepreneurship (IHEIE), 75006 Paris, France

E-mail: regis.bisson@univ-amu.fr

Keywords: deuterium, ammonia, stainless steel, 316L, desorption, plasma-wall interactions

OPEN ACCESS

RECEIVED
30 June 2023

REVISED
31 January 2024

ACCEPTED FOR PUBLICATION
20 February 2024

PUBLISHED
29 February 2024

Abstract

We present a systematic study that quantifies deuterium (D) retention and ammonia (ND_3) production from 316 L stainless steel (SS316L) following the implantation of D ions in conditions similar to the ones expected in the ITER tokamak, i.e. with kinetic energy below 300 eV. Using Temperature Programmed Desorption (TPD) after deuterium ion implantation at 250 eV/D, we show that deuterium retention increases linearly with the D fluence up to 10^{21} D^+m^{-2}, with a retention probability of 18%. For higher D fluence, deuterium retention increases sub-linearly. Analysis of the TPD spectra evolution with varying storage time in vacuum after D implantation, shows that D retention is influenced by D diffusion into the bulk of SS316L. Subsequent to D ion implantation, we evidence the efficient production of ND_3 molecules during TPD, between 400 K and 750 K, from the nitrogen present naturally in SS316L. Up to 21% of the D release during TPD can be found in ND_3 molecules, indeed. The fraction of ND_3 in the total D release depends both on the D ion fluence and the nitrogen concentration profile in the bulk. At least 7% of the D release is found in the form of ND_3 molecules, even at a fluence of 2×10^{21} D^+m^{-2} and for a natural N concentration bulk profile. Both N diffusion and D diffusion into the bulk appear to dictate the kinetics of ND_3 production. Our findings of efficient production of ND_3 in D-implanted austenitic 316 L stainless steel underline the need for similar studies on reduced-activation ferritic/martensitic (RAFM) steels that contain similar content of nitrogen and will be used in fusion reactor prototypes.

1. Introduction

The international experimental fusion reactor ITER is currently under construction in Cadarache (France). This tokamak will fuse a mixture of hydrogen isotopes, deuterium (D) and radioactive tritium (T), at ion temperatures of ~10 keV, producing energetic ~100 keV He ions and ~14 MeV neutrons. High energy ions are confined in ITER's vacuum vessel with intense magnetic fields to avoid keV ion implantation and sputtering of plasma-facing component (PFC) tiles, made of tungsten, which protect the vacuum vessel. Nevertheless, PFC tiles are also expected to be impinged by a large range of neutral flux from 10^{19} to 10^{24} $m^{-2}s^{-1}$ with typical kinetic energy <300 eV [1]. 316 L stainless steel (SS316L) is the material used for the vacuum vessel as well as for the structures attaching PFC tiles to the vacuum vessel. Thus, SS316L surfaces within the instruments and diagnostics ports as well as the gaps between the PFC tiles, will be subjected to <300 eV deuterium and tritium implantation. It was estimated for ITER that the SS316L surface area subjected to neutral hydrogen isotopes implantation could represent about 8% of the surface of the vessel [2]. Tritium inventory is an important consideration for D-T fusion plasma reactors such as ITER, since nuclear regulation imposes a limited quantity of (trapped) tritium in the reactor at any given time. Therefore, an extensive literature exists onto the topic of hydrogen isotope retention in and release (desorption) from 316 and 316 L stainless steels [2–8]. SS316L is a fcc austenitic alloy with a composition (expressed in the remainder of the text in wt. %) majorly made up Fe

(>60%), Cr (16%–18%), Ni (10%–12%), Mo (2%–3%), Mn (2%), and a small amount of N (<0.1%). For ITER, specific variants of 316L have been developed, generally called 316L(N)-IG with L indicating a reduced C content, (N) a controlled N content and IG standing for ITER-Grade. The main purpose of SS316L(N)-IG is to reduce its nuclear activation during D-T fusion plasma and, notably in the context of the present study, the specified nitrogen (N) content lies between 0.06 and 0.08%. The operating temperatures of these SS316L structural materials are expected to vary between 350 K and 573 K [9].

Ghiorghiu *et al* have shown recently that deuterium ion implantation in N-implanted tungsten (W) leads to the production of deuterated ammonia for surface temperatures between 350 K and 650 K [10]. Considering that SS316L contains significant amounts of nitrogen, that its operational temperature falls within the temperature range of ammonia production on W, that iron (Fe) is at the basis of the industrial production of ammonia with the Haber–Bosch process [11] and that, once produced, ammonia adsorbs on ITER's materials [12], it is timely to investigate for tritium inventory issues how efficient ammonia production could be when SS316L is implanted with hydrogen isotopes. To the best of our knowledge, ammonia production from the natural N content of SS316 or SS316L has never been reported in the literature. Therefore, the following literature review on deuterium retention and release from SS316 does not account for the possible ND_3 release in thermodesorption experiments.

In the late 1970s, a series of studies on deuterium retention in SS316 were conducted in preparation of the D-T fusion plasma of the TFTR tokamak. Altstetter *et al* implanted 7 keV/D^+ ions at room temperature in SS316. The deuterium ions were implanted with fluxes of 10^{17}–10^{19} $D^+m^{-2}s^{-1}$, while the time integrated ion implantation (fluence) varied from 10^{19} to 10^{23} D^+m^{-2}. The subsequent D retention in the near-surface of SS316, within 400 nm, was measured by Nuclear Reaction Analysis (NRA). Immediate post-implantation measurements showed a linear increase in D retention up to a fluence of 10^{21} D^+m^{-2}, with a retention probability of about 88% of the implanted fluence. However, for a delayed quantification of D retention (2 h post implantation, the so-called storage time of 2 h hereafter) the apparent D retention decreased by a factor of ~2 [4]. Altstetter *et al* proposed that part of the implanted D had been released to the vacuum and the remainder part had diffused in the SS316 bulk, deeper than the 400 nm probed by NRA. Wilson and Baskes [5] implanted SS316 at 296 K with 333 eV/D^+ ions at a flux of 10^{19} $D^+m^{-2}s^{-1}$ and for a fluence of 3×10^{22} D^+m^{-2} and analysed the D release by Temperature Programmed Desorption (TPD) after 1 h of storage time at 296 K. They observed a deuterium desorption peak at 400 K with a desorption tail up to 550 K. The desorption peak shifted to a higher temperature by 60 K when increasing the fluence 100-folds, i.e. by increasing the implantation duration from a couple of minutes to several hours. Furthermore, the single desorption peak reduced in intensity and split in two desorption peaks at 380 K and 430 K when increasing the storage time to 21.5 h [7]. They interpreted these results by the combined effect of partial D release to the vacuum and efficient diffusion in the bulk, with the two desorption peaks ascribed to, respectively, release from a near-surface trap and bulk diffusion. Finally, Wilson and Baskes observed that for D ions fluences $<10^{21}$ D^+m^{-2}, deuterium retention probability is higher than at larger fluence, consistent with Altstetter *et al* measurements, and they argued that this could be an effect of the oxide layer of SS316.

Detailed N retention studies in SS316 and 316 L started in the 1980s due to the growing interest in steel nitriding technologies. Hirvonen and Anttila [13] implanted 40 keV/N^+ in SS316 with a flux of 3×10^{17} $N^+m^{-2}s^{-1}$ and a fluence of 7.5×10^{20} N^+m^{-2}. Nuclear Resonant Broadening was used to characterize N diffusion into the bulk after various annealing between 673 K and 773 K. The diffusion activation energy of N in SS316 was determined to be 1.87 eV, higher than the 1.27 eV found for pure Fe, with both materials having a similar pre-exponential factor of ~0.05 cm^2s^{-1}. Additionally, they showed that at a brief 5 min annealing at 773 K was sufficient for the edge of the N concentration profile to diffuse by several tens of nm. Martinavicius *et al* implanted 250–500 eV/N^+ beam in SS316L single crystals with a flux of 5×10^{19} $N^+m^{-2}s^{-1}$ and a fluence of 1.7×10^{23} N^+m^{-2} at a temperature between 643 K and 703 K and measured the resulting N profile in the bulk with NRA. The diffusion activation energy was found to vary between 1.1 and 1.4 eV, depending on single crystal orientation, with pre-exponential factor varying between, respectively, 0.001 and 0.05 cm^2s^{-1} [14]. These studies show that nitrogen diffusion is efficient in SS316L at ~640 K, even at low implantation flux and low fluence. These observations in SS316L are reminiscent of the earlier work of Bozso *et al* [15] conducted on Fe(100) and Fe(111) single crystals, which showed that nitrogen diffusion in the bulk from the surface of iron is efficient at 640 K, even though nitrogen desorption sets in at ~750 K.

In the present work, we first measure deuterium retention and release from SS316L, to check that the knowledge gathered on SS316 is still valid on the low carbon content SS316L. We then characterize nitrogen desorption from SS316L to ensure that experimental conditions can be found where a single SS316L sample can be used to measure systematically both deuterium release and the eventual generation of deuterated ammonia. Finally, we quantify how much ammonia is produced from SS316L as well as N-implanted SS316L, comparing the obtained results with N-implanted W to shed light on the ammonia formation mechanism in SS316L. This

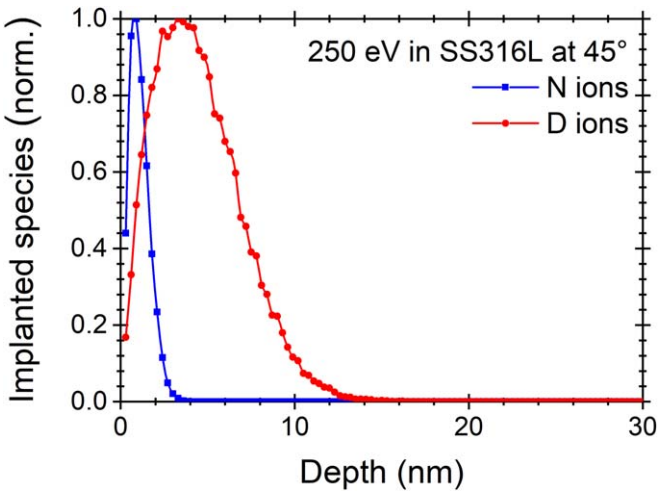

Figure 1. Normalized SRIM implantation profile for 250 eV N (blue squares) and D ions (red circles) impinging at 45° on a proxy SS316L material.

paper concludes with a summary and a perspective for future studies that could further improve the knowledge about ammonia production from steels used for ITER and future reactors like DEMO.

2. Experimental methods

Samples were cut from a 500 μm thick foil provided by Goodfellow as annealed and polished AISI 316 L with the following specified content: 18% Cr, 10% Ni, 3% Mo, C < 0.03%. According to the AISI standard, other chemical components in SS316L must be Fe > 60%, Mn < 2.0%, Si < 1.0%, N < 0.1%, P < 0.045% and S < 0.03%. According to ASTM A480, the SS316L foil was solution annealed to 1313 K and quenched at a rate sufficient to prevent reprecipitation of carbides. Ion implantation and TPD experiments were conducted in an experimental apparatus featuring two interconnected ultra-high vacuum (UHV) chambers: a load-lock/storage chamber (base pressure $< 3 \times 10^{-9}$ mbar) and an implantation/TPD chamber (base pressure $< 2 \times 10^{-9}$ mbar). The load-lock/storage chamber is used to introduce the sample from air to UHV and then to store the ion-implanted samples during the preparation of TPD. The implantation/TPD chamber is equipped with an OMICRON ISE 10 ion source for ion implantation and with a PID-controlled radiative oven located 2 mm below a differentially pumped chamber (base pressure $< 1 \times 10^{-10}$ mbar) containing a quadrupole mass spectrometer (HIDEN 3F/PIC, noted QMS in the following) in order to perform TPD measurements. We summarize here the experimental protocol followed in this study, the detailed protocol can be found in [10]. The ion source produced D_2^+ or N_2^+ ions accelerated to a kinetic energy of 500 eV. Thus, most ion fragments passing the surface are assumed to have a kinetic energy of 250 eV per nucleus. Ions impinge the sample with an incidence angle of 45° and the implantation range of the ensuing 250 eV D and N fragments are estimated with the binary collision code SRIM [16] on a proxy amorphous material composed of 66% Fe, 18% Cr, 10% Ni, 3% Mo, 2% Mn and 1% Si, to be, respectively, 4.34±2.47 nm and 0.97±0.57 nm (figure 1). A single ion source has been used to ensure an optimal overlap of the two ions beam footprints on the SS316L samples and a thorough pumping/degassing procedure of the ion source is performed when switching the gas feed, with the SS316L samples located in the load-lock/storage chamber.

Once introduced in the load-lock/storage chamber from air and before systematic deuterium implantation/TPD experiments were performed, SS316L samples were subjected to a degassing procedure consisting of at least two linear temperature ramps of 1 Ks^{-1} up to 800 K, unless stated otherwise. This procedure stabilizes the surface of SS316L samples as will be discussed in section 3.1. All ion implantations are realized at 300 K. D implantation is realized at a constant flux of $\sim 2.2 \times 10^{16}$ $D^+m^{-2}s^{-1}$ for a given duration to reach the desired D fluence. A sequential co-implantation/TPD experiment consists in first implanting the SS316L sample with N ions at a constant flux of $\sim 1.9 \times 10^{16}$ $N^+m^{-2}s^{-1}$ for a determined duration to obtain the desired N fluence. During TPD, the sample temperature is increased linearly with a ramp of 1 Ks^{-1} and its value is recorded simultaneously with the desorption rates measured by the multiplexed QMS at m/z = 3, 4, 20 and 28 for HD, D_2, ND_3 and N_2 products, respectively. The entrance of the QMS chamber is located 2 mm above the sample, the ionization head of the QMS being in the line of sight with the centre of the sample. Thus, every desorbing molecule is detected by the QMS without prior collision with a chamber wall ensuring that the relative

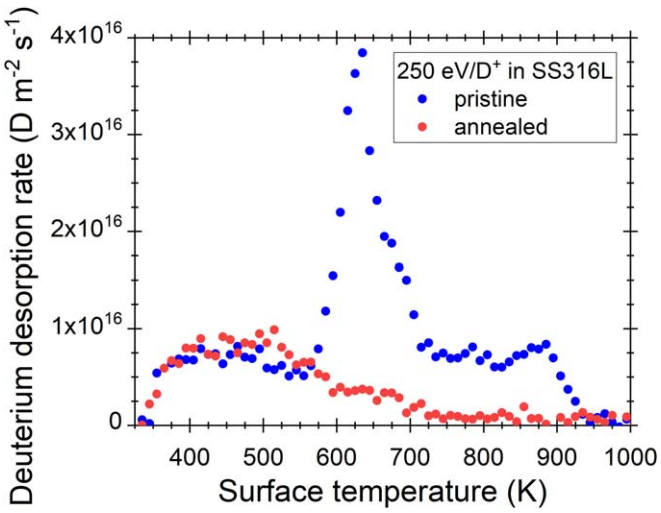

Figure 2. Deuterium desorption from pristine SS316L (blue circles) and 1250 K-annealed SS316L (red circles).

probability of detection of different desorption products, like molecular deuterium and deuterated ammonia, is solely defined by the ratio of their ionization probability and not by their different reflection and adsorption probability on vacuum chamber walls [17]. To optimize the ion implantation/TPD measurements, six samples were used to study the thermal evolution of SS316L samples (section 3.1) and three SS316L samples were used to optimize the deuterium release/retention and the ammonia production measurements (section 3.2 and section 3.3, respectively), giving consistent results. Finally, one SS316L sample was used to obtain the results presented in sections 3.3 and 3.4. Error bars represent the standard deviation of the mean of replicate measurements performed systematically on this last SS316L sample.

3. Results and discussion

3.1. Thermal evolution of 316L stainless steel and its effect on deuterium release

The thermal stability of SS316L samples has been studied with x-ray Photoelectron Spectroscopy (XPS), to follow the surface chemical composition, and with the line-of-sight QMS to register the desorption of the alloy elements. Detailed results are presented in [18] and a brief summary is given here. The surface of the as-introduced SS316L samples (pristine SS316L hereafter) contains 90% of oxidized Fe and 10% of oxidized Cr. Upon thermal annealing up to 1250 K, one observes at ~550 K the onset of desorption of several alloy elements (Fe, Cr, CrO, Ni and Mn) which is concomitant with the onset of Cr diffusion through FeO_x oxides [19]. The desorption from the sample arrives at a minimum around ~750 K, where the surface composition of SS316L evolved to 35% of partially reduced Fe and 55% of oxidized Cr. The remaining 10% elemental composition is made of metallic Ni and oxidized Mn. Then at ~875 K, an important Mn desorption occurs leading to a further Mn oxide surface enrichment and the appearance of Cr metal. The thermal evolution of the SS316L surface composition upon annealing is irreversible and has an important effect on deuterium retention and release.

Figure 2 presents the deuterium release from a single SS316L sample that was implanted with deuterium twice at 2.8×10^{19} D^+m^{-2}: once after introduction in UHV of the pristine sample and once after annealing of the sample to 1250 K. Pristine SS316L exhibits three D desorption features. The onset of the first desorption feature is at ~330 K and it peaks at ~450 K. The second desorption feature starts to rise at 575 K and peaks at 630 K. Finally, another peaking of deuterium desorption is observed around 875 K. In contrast, annealed SS316L has a simpler D desorption behavior with an onset of desorption around ~330 K, a desorption peak at 450 K and a desorption shoulder up to ~700 K. Comparing these two measurements, we attribute the two high-temperature D desorption peaks at 630 K and 875 K to the evolution of the surface oxide of SS316L. The former is related to the chromium oxide enrichment at the surface, and the latter to the manganese oxide formation and the partial reduction of Cr as shown by XPS [18]. Thus, we conclude that the low-temperature D desorption peak at 450 K is related to deuterium retention in the near-surface and bulk of SS316L, similar to the observation of Wilson and Baskes [5]. Note that the ~50 K difference in desorption peak temperature between Wilson and Baskes and the present study could be related to differences in the method for surface temperature measurement. In the present study, the type-K thermocouple is spot-welded on the oven close to the sample and

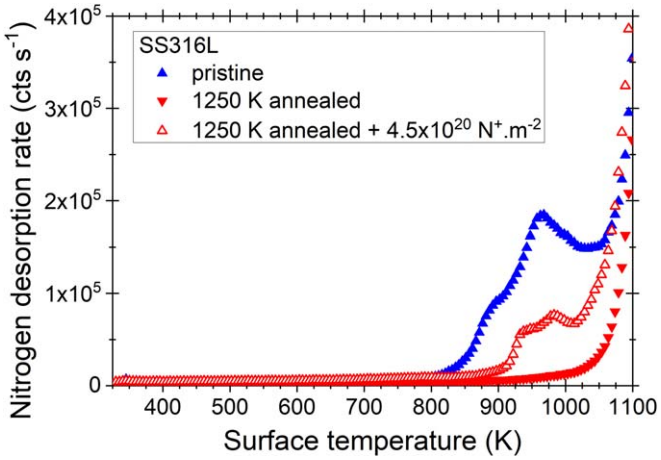

Figure 3. Nitrogen desorption from a SS316L sample. Nitrogen atoms naturally present in the bulk of SS316L are desorbing above 800 K (full blue triangles). Implanted N ions are desorbing in the same temperature range (open red up triangles).

the sample temperature is obtained through calibration, while Wilson and Baskes directly spot-welded thermocouples on their samples.

3.2. Nitrogen desorption from 316 L stainless steel

Since AISI SS316L samples contain nitrogen and this study aims at evaluating the possibility to form ammonia from D-implanted SS316L, we characterized the N desorption temperature.

Figure 3 presents raw nitrogen desorption measurements performed with the $m/z = 28$ channel of the QMS. A large amount of desorption at $m/z = 28$ is found from pristine SS316L above 825 K, with desorption peaks around ~900 K and ~950 K. However, 1250 K-annealed SS316L does not show any desorption peak below 1050 K. To confirm that the desorption observed above 825 K on the $m/z = 28$ channel is related to nitrogen desorption and not carbon monoxide (from the heated oven), a nitrogen ion implantation with a fluence of 4.5×10^{20} N^+m^{-2} was realized in the annealed SS316L sample. It is found that N-implanted annealed SS316L also exhibits two desorption peaks at ~925 K and ~975 K, similar to the pristine sample and the observation of Bozso *et al* on Fe single crystals [15]. Note that the apparent shift of 25 K for natural N desorption and implanted N desorption is likely related to the usual oven temperature reproducibility we observe at high temperature. The quantity of natural N released from pristine SS316L up to 1100 K is similar for several samples and it is about three times higher than the 4.5×10^{20} N^+m^{-2} implanted here. Considering the nitrogen implantation probability of 69% obtained with SRIM on a pure Fe material in the present implantation conditions and by comparing the amounts of N desorption from pristine SS316L and N-implanted annealed SS316L, we determine that about 9×10^{20} Nm^{-2} of natural N was desorbed from pristine SS316L when annealed at 1 Ks^{-1} to ~1100 K, i.e. only 0.08% of the total N natural content of the present SS316L sample (assuming a N content similar to SS316L(N)-IG). The remaining natural N content likely desorbs above 1100 K, as suggested by the rapidly increasing $m/z = 28$ signal above 1050 K in figure 3 and as it was observed by Bozso *et al* on pure Fe [15], i.e. the remaining natural N content is coming from deeper in the bulk.

3.3. Deuterium retention in 316 L stainless steel

In section 3.1, we showed that SS316L must be annealed once above 700 K to ensure the stabilization of its surface oxide for further TPD analysis. In section 3.2, we found that the desorption of the natural content of nitrogen from the near surface of SS316L occurs above 825 K. Therefore, to systematically study the retention and release of D in SS316L and the potential production of ammonia we employed the following strategy. We introduced a pristine SS316L into the UHV setup and realized two TPD ramps up to 800 K. This sample preparation stabilizes the SS316L surface oxide and prevents the desorption of its natural N content. Then, we performed a series of D implantations at 300 K followed by TPD ramps up to 800 K on the same 800 K-annealed sample (annealed, hereafter). We varied the D ion fluence or the storage time in vacuum to investigate their effects on D retention and release. Each experimental condition is repeated two to three times to estimate error bars with the standard deviation of the mean and evaluate the reproducibility of replicate measurements. The average relative error is 24% on replicate measurements.

Figure 4 displays the integration of the deuterium release up to 800 K, i.e. the evaluation of the deuterium retention by TPD, for annealed SS316L implanted with 2.8×10^{19} D^+m^{-2} with different storage times in vacuum at 300 K. We observe that deuterium retention in SS316L is reduced by 45% when the storage time is

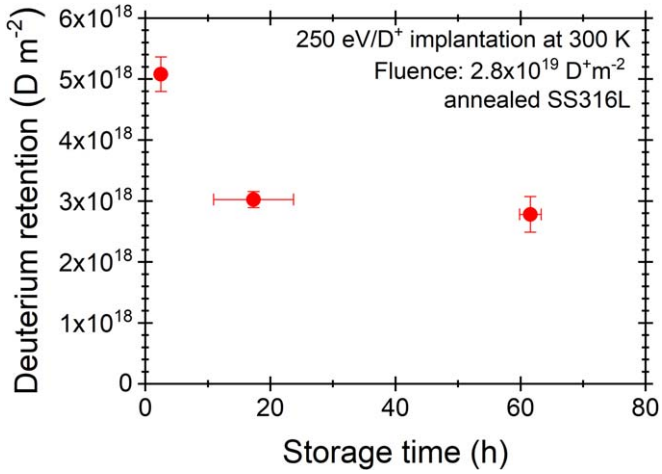

Figure 4. Deuterium retention in 800 K-annealed SS316L as a function of storage time in vacuum.

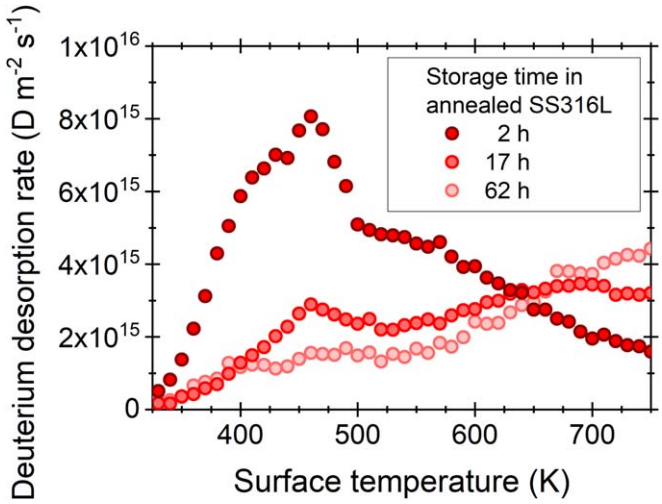

Figure 5. Deuterium release after 2.8×10^{19} $D^{+}m^{-2}$ implantation in 800 K-annealed SS316L as a function of sample temperature for three different storage time after the end of the D implantation.

increased from 2 h to 62 h. This result obtained on SS316L at low fluence (10^{19} $D^{+}m^{-2}$) is similar to the observations made by Altstetter *et al* and Wilson and Baskes on SS316 at higher fluence ($10^{21\text{-}22}$ $D^{+}m^{-2}$). We note that similar dynamic retention was obtained in similar experimental conditions on a batch of polycrystalline W samples, which were analyzed as the result of a competition between bulk diffusion, trapping in the surface oxide and desorption to the vacuum [20].

A signature of bulk diffusion in SS316L is discernible in the TPD spectra obtained at various storage times presented in figure 5. When the storage time after D implantation increases from 2 h to 62 h, a decrease in the intensity of the 450 K deuterium desorption peak is observed, while the high temperature shoulder appears to shifts to higher temperatures. Such behavior is also noticeable in figure 4 of Wilson and Baskes TPD measurements [5], although it was not discussed in their work. In line with Wilson and Baskes' analysis, the low-temperature peak is associated with a near-surface trap, while the high-temperature peak/shoulder is related to bulk diffusion. We propose that the reduction of the 450 K peak is due to the release of deuterium initially trapped in the vicinity of the SS316L surface oxide into vacuum, i.e. a near-surface trap reminiscent of the native oxide of tungsten [20]. The shift of the high-temperature desorption shoulder to higher temperature is likely due to the release of deuterium located deeper within the bulk, following diffusion during the storage time. An important consequence of this storage time effect, which shifts the desorption of some implanted D to higher temperature, is the possibility of underestimating D retention from TPD measurements interrupted at 800 K. Therefore, in the following study we will restrict the storage time to about 2 h in order to minimize the underestimation of D retention.

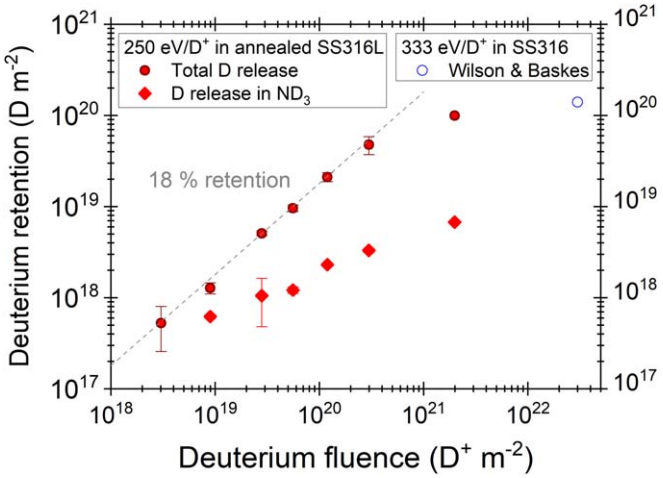

Figure 6. Deuterium retention in 800 K-annealed SS316L as a function of D ion fluence (full red circles). The fraction of deuterium released during TPD as deuterated ammonia molecules is shown with full red diamonds. Deuterium retention measured in SS316 by Wilson and Basked is shown with an open blue square [7].

Figure 6 displays the evolution of D retention in D-implanted SS316L as a function of D ion fluence. Note that this evaluation of D retention includes the deuterium released in the form of D_2, HD and deuterated ammonia (ND_3) molecules, the latter being discussed in section 3.4. As the D ion fluence increases, one observes a linear increase in D retention, similar to the NRA study of Altstetter *et al* [4]. The apparent retention probability is 18% of the implanted flux in our experimental conditions. However, when the D ion fluence is above 10^{21} D^+m^{-2} one observes that the retention probability becomes sublinear, consistent with Wilson and Baskes' observation [5] as shown with the open blue circle in figure 6 [7]. A sublinear dependency of D retention with D ion fluence is generally attributed to a combined effect of the saturation of near-surface traps and bulk diffusion [20]. The present observation of the D fluence regime where sub-linearity in deuterium retention appears could be used to estimate the density of the near-surface traps in 800 K-annealed and surface-stabilized SS316L. Note that the quantitative consistency of our deuterium retention measurements with the one of Wilson and Baskes stands from the fact that the fraction of deuterium released as deuterated ammonia is only in the percent range for the fluence range $> 10^{21}$ D^+m^{-2}, as it will be discussed now in the next section.

3.4. Ammonia production from 316L stainless steel

As can be seen in figure 6, significant amounts of ND_3 molecules have been measured during the TPD evaluation of D retention from D-implanted SS316L. Figure 7 shows that the fraction of D release found in ND_3 products is up to 21% in the 10^{19} D^+m^{-2} fluence range, and then gradually decreases down to 7% for fluence above 10^{21} D^+m^{-2}. The consistent measurement of several 10^{18} ND_3 m^{-2} molecules for each D implantation/TPD measurements after a deuterium ion fluence $> 10^{20}$ D^+m^{-2} (figure 6, full red diamonds) implies that the nitrogen present naturally in SS316L easily diffuses to the surface and efficiently recombines with D atoms diffusing from the bulk. The total amount of ND_3 molecules produced from the SS316L sample used to realize figures 6 and 7 is on the order of 1×10^{19} ND_3 m^{-2}, which is comparable to the SS316L surface atom density. The absence of any decrease in ND_3 production for replicate measurements indicates that the source of natural N is far from being depleted during these experiments.

Figure 6 shows that the amount of ND_3 molecules produced during a TPD ramp does not saturate with the D ion fluence, at least up to $\sim 2 \times 10^{21}$ D^+m^{-2}. This observation on SS316L is at variance with the results obtained on N-implanted polycrystalline W by Ghiorghiu *et al* [10] where ND_3 production saturation was occurring for D ion fluences $> 10^{20}$ D^+m^{-2}. Ghiorghiu *et al* attributed the observed ND_3 production saturation to the absence of N diffusion to the surface of W below 800 K, thus only N atoms already present at the surface before the TPD ramp can produce ND_3 molecules. We note that on annealed W, deuterium desorption stops at 700 K, i.e. before N diffusion sets in, and that both the maximum desorption rate of ND_3 and D_2 occur at the same temperature on W. This behavior is consistent with D_2 diffusion to the surface being the rate-limiting step for ND_3 production on W, since N diffusion is inactive below 800 K in N-implanted W.

On SS316L, the ND_3 production kinetics seems to be less constrained than on W. Figure 8 presents the ND_3 production rate from SS316L (full red diamonds) for a D ion fluence of 3×10^{20} D^+m^{-2}. One observes that ND_3 release sets up at ~375 K, reaches a maximum rate in the 550 K—600 K range and significant quantities of ND_3 are still produced above 700 K. The ND_3 maximum production rate on SS316L (550 K—600 K) occurs at a higher

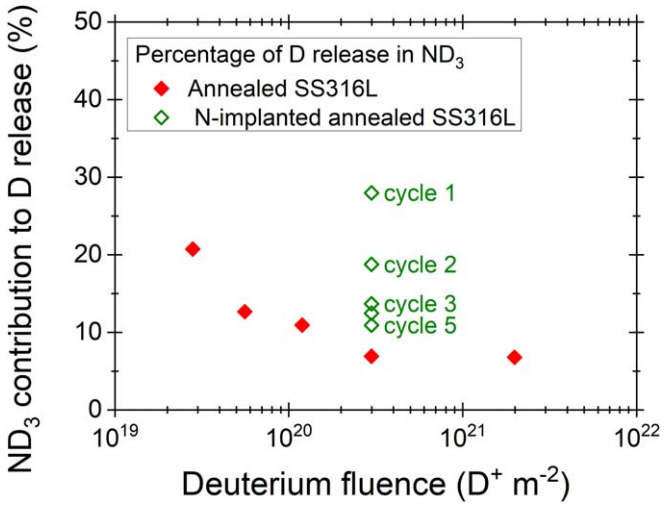

Figure 7. ND_3 contribution to the total deuterium release during TPD obtained after D ion implantation in 800 K-annealed SS316L as a function of deuterium ion fluence. Full red diamonds correspond to ND_3 production from the natural nitrogen content of SS316L. Open green diamonds are measurements obtained for successive D implantation/TPD in a N-implanted 800 K-annealed SS316L with an ion fluence of 4.5×10^{20} N^+m^{-2}.

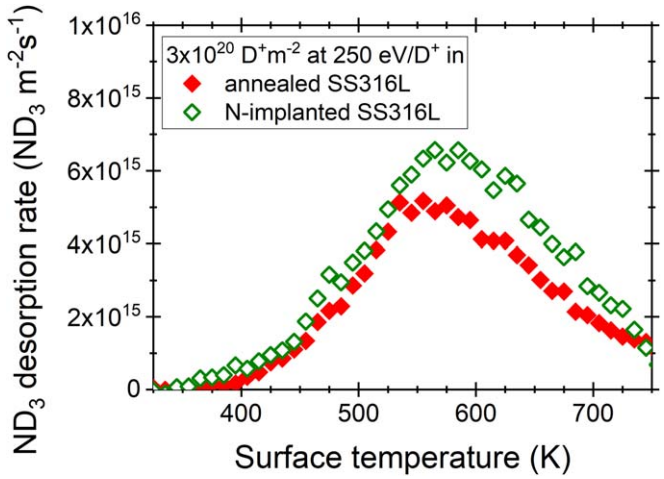

Figure 8. ND_3 release from 800 K-annealed SS316L as a function of sample temperature after a 3×10^{20} D^+m^{-2} implantation. N-implanted 800 K-annealed SS316L were subjected to a 4.5×10^{20} N^+m^{-2} implantation prior D implantation.

surface temperature than the D maximum release rate (450 K, figure 5), in stark contrast to N-implanted W. This observation suggests that D diffusion to the surface of SS316L is not the rate limiting step for ND_3 production. Instead, we propose that the kinetics of ND_3 production on SS316L are determined by both D diffusion and N diffusion to the surface.

In order to test the role of N diffusion in ND_3 production, we implanted 4.5×10^{20} N^+m^{-2} in 800 K-annealed SS316L prior to implanting a D ion fluence of 3×10^{20} D^+m^{-2}. Figure 8 shows that subsequent to this sequential N+D implantation, the ND_3 production increases by ~32%, indeed. This increase in ND_3 production is in agreement with the observed ratio of implanted N versus natural N in SS316L shown in figure 3. Therefore, it seems that natural N and implanted N have roughly the same efficiency for ND_3 production. We note that the increased ND_3 production from implanted N seen in figure 8 occurs for a surface temperature > 550 K, consistent with the literature on N diffusion [13, 14]. All in all, these observations are consistent with N diffusion being an important player in the kinetics of ND_3 production from SS316L.

Finally, in order to test if nitrogen seeding of fusion edge plasma [21, 22] could contribute to an increased production of ND_3 from SS316L, we repeated several times the 3×10^{20} D^+m^{-2} implantation/TPD measurement cycle onto the 4.5×10^{20} N^+m^{-2} implanted SS316L sample. Figure 7 shows that the fraction of ND_3 in D release is initially increased to 28%. Then it takes about 5 cycles for the ND_3 fraction in D release to come back in the 10% range. The smearing of the N concentration profile into the bulk of SS316L through

thermally-assisted diffusion is likely responsible for the observed rapid decrease of ND_3 production enhancement following N-implantation.

4. Summary and perspectives

We evidenced that the surface composition of 316L stainless steel has a strong influence on its deuterium retention and release. By limiting the annealing of SS316L to 800 K, we were able to stabilize its surface composition to 35% Fe and 55% Cr oxides and to obtain reproducible D retention and release measurements. Consistent with the literature on SS316 [4, 5, 7], we found that D bulk diffusion in SS316L is significant at 300 K over the course of a day. The observed transition from a linear dependency of D retention with D fluence to a sublinear dependency above 10^{21} D^+m^{-2} is attributed to the saturation of the near-surface traps related to the surface oxides.

We demonstrated that the natural nitrogen content of SS316L leads to the production of ND_3 molecules in significant quantities. ND_3 production represents more than 20% of the D release during TPD for D ion fluence in the 10^{19} D^+m^{-2} range and about 7% of the D release in the 10^{21} D^+m^{-2} range. The amount of ND_3 molecules increases continuously with the D ion fluence, i.e. without saturation, in stark contrast with previous observations made on N-implanted W. It is well-known that N does not diffuse in W below 800 K, but that N does diffuse efficiently at ~640 K in SS316L. The temperature at which the maximum of ND_3 production occurs in TPD is higher by 100–150 K than the D_2 release temperature, pointing to kinetics for ND_3 production from SS316L sensitive to both D diffusion and N diffusion.

The present results are of importance for quantifying the production of tritiated ammonia in the ITER tokamak, even in the absence of nitrogen seeding of fusion edge plasma. We have demonstrated that tritiated ammonia is to be expected from non-shadowed SS316L surfaces of the vacuum vessel and from the gaps between the PFC tiles, indeed. We note that future fusion reactor prototypes like DEMO will replace SS316L with reduced-activation ferritic/martensitic (RAFM) steel such as EUROFER [23], that still contains nitrogen in the 0.02–0.04 wt% range. Thus, we hope that the present study will raise attention to the issue of tritiated ammonia production from the natural N content of RAFM steel.

Acknowledgments

The project leading to this publication has received funding from Excellence Initiative of Aix-Marseille University - A*MIDEX, a French Investissements d'Avenir programme. We thank the financial support of the French Federation for Magnetic Fusion Studies (FR-FCM). Part of this work has been carried out within the framework of the EUROfusion Consortium and has received funding from the Euratom research and training programme 2014–2018 and 2019–2020 under grant agreement No 633053. The views and opinions expressed herein do not necessarily reflect those of the European Commission. Work performed under EUROfusion WP PFC. The views and opinions expressed herein do not necessarily reflect those of the ITER Organization. ITER is the Nuclear Facility INB no. 174. This paper applies new physics analysis related to tritiated ammonia formation, which is not yet incorporated into the ITER technical baseline. The nuclear operator is not constrained by the results presented here.

Data availability statement

All data that support the findings of this study are included within the article (and any supplementary files).

ORCID iDs

M Minissale https://orcid.org/0000-0001-6331-1402
R Bisson https://orcid.org/0000-0002-8819-1563

References

[1] Roth J *et al* 2009 Recent analysis of key plasma wall interactions issues for ITER *J. Nucl. Mater.* **390** 1
[2] Houben A *et al* 2020 Hydrogen permeation and retention in deuterium plasma exposed 316L ITER steel *Nucl. Mater. Energy* **25** 100878
[3] Wilson K L, Thomas G J and Bauer W 1976 Low-energy proton implantation of stainless steel *Nucl. Technol.* **29** 322
[4] Altstetter C J, Behrisch R, Bøttiger J, Pohl F and Scherzer B M U 1978 Depth profiling of deuterium implanted into stainless steel at room temperature *Nucl. Instrum. Methods* **149** 59
[5] Wilson K L, Baskes M I and Deuterium T 1978 lN irradiated 316 stainless steel *J. Nucl. Mater.* **76–77** 291

[6] Blewer R S, Behrisch R, Scherzer B M U and Schulz R 1978 Trapping and replacement of 1–14 keV hydrogen and deuterium in 316 stainless steel *J. Nucl. Mater.* **76–77** 305
[7] Wilson K L and Baskes M I 1978 Thermal desorption of deuterium-implanted stainless steel *J. Nucl. Mater.* **74** 179
[8] Nemanič V, Žumer M and Zajec B 2008 Deuterium retention in ITER-grade austenitic stainless steel *Nucl. Fusion* **48** 115009
[9] Kalinin G, Gauster W, Matera R and Tavassoli A-A F 1996 Structural materials for ITER in-vessel component design *J. Nucl. Mater.* **233–237** 9
[10] Ghiorghiu F *et al* 2021 Nitrogen retention and ammonia production on tungsten *Nucl. Fusion* **61** 126067
[11] Ertl G 2008 Reactions at surfaces: from atoms to complexity (nobel lecture) *Angew. Chem. Int. Ed.* **47** 3524
[12] Minissale M *et al* 2020 Sticking probability of ammonia molecules on tungsten and 316L stainless steel *Surfaces, J. Phys. Chem.* C **124** 17566
[13] Hirvonen J and Anttila A 1985 Annealing behavior of implanted nitrogen in AISI 316 stainless steel *Appl. Phys. Lett.* **46** 835
[14] Martinavičius A, Abrasonis G and Möller W 2011 Influence of crystal orientation and ion bombardment on the nitrogen diffusivity in single-crystalline austenitic stainless steel *J. Appl. Phys.* **110** 074907
[15] Bozso F, Ertl G, Grunze M and Weiss M 1977 Interaction of nitrogen with iron surfaces *J. Catal.* **49** 18
[16] Ziegler J F, Ziegler M D and Biersack J P 2010 SRIM—The stopping and range of ions in matter (2010) *Nucl. Instrum. Methods Phys. Res. Sect. B Beam Interact. Mater. At.* **268** 1818
[17] Bisson R *et al* 2015 Dynamic fuel retention in tokamak wall materials: An *in situ* laboratory study of deuterium release from polycrystalline tungsten at room temperature *J. Nucl. Mater.* **467** 432
[18] Louis De Canonville C *et al* 2023 Optical properties, surface composition and desorption of Stainless Steel (316L) studied from ambient temperature to 1000 K in vacuum *Mater. Today Commun.* **36** 106865
[19] Asami K, Hashimoto K and Shimodaira S 1978 Changes in the surface compositions of FeCr alloys caused by heating in a high vacuum *Corros. Sci.* **18** 125
[20] Hodille E A *et al* 2017 Retention and release of hydrogen isotopes in tungsten plasma-facing components: the role of grain boundaries and the native oxide layer from a joint experiment-simulation integrated approach *Nucl. Fusion* **57** 076019
[21] Kallenbach A *et al* 2010 Divertor power load feedback with nitrogen seeding in ASDEX Upgrade *Plasma Phys. Control. Fusion* **52** 055002
[22] Giroud C *et al* 2013 Impact of nitrogen seeding on confinement and power load control of a high-triangularity JET ELMy H-mode plasma with a metal wall *Nucl. Fusion* **53** 113025
[23] Lindau R *et al* 2005 Present development status of EUROFER and ODS-EUROFER for application in blanket concepts *Fusion Eng. Des.* **75–79** 989